3

Thermoelectric Phenomena under Large Temperature Gradients

L.I. Anatychuk
Institute of Thermoelectricity

L.P. Bulat
St. Petersburg State University of Refrigeration

3.1 Introduction

Recent decades have witnessed numerous experimental procedures for creating a very sharp spatial temperature inhomogeneity in various materials. Thus, temperature gradients of up to 10^{10} K/cm can be established by laser radiation on semiconductors, electron-beam material processing, welding, etc. Large electron temperature gradients can also be achieved by heating up semiconductor charge carriers with microwave field[1,2]; hence the relevance of investigation into semiconductor properties under large temperature gradients.

The tendency toward miniaturization of thermoelectric power converters also leads to the creation of large temperature gradients in semiconductor materials. Consequently, the task arises to study transport phenomena in semiconductors under extreme temperature conditions. This situation will arise in the use of submicron and nanosize structures as thermoelectrics. Thus, in a thermoelectric generator based on a quantum super lattice, for example, temperature gradients up to 10^5 K/cm are established.[3] Under these conditions, an extremely high thermoelectric figure-of-merit was obtained: $ZT = 2.4$ at $T = 300$ K.[3]

In addition, new effects can be expected under large temperature gradients. One is the Benedicks effect,[6] which has been described in a number of experimental and theoretical papers.[2] The origin of

© 2006 by Taylor & Francis Group, LLC

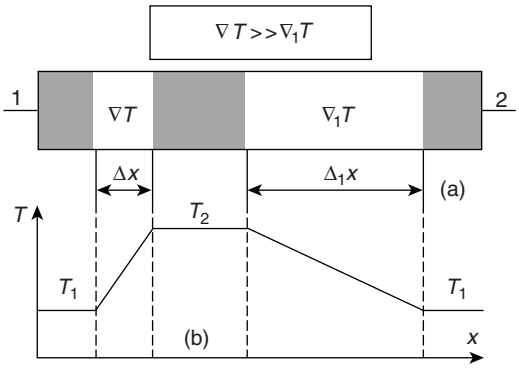

FIGURE 3.1 Conditions of the Benedicks effect observation: (a) sample shape, (b) temperature distribution $T(x)$ along the sample.

this effect lies in the thermo-electromotive force (EMF) in a homogeneous isotropic sample where two opposite temperature gradients of different values are created — the ends of the sample being maintained at equal temperature (Figure 3.1).

In this chapter the mechanisms of the effect of a temperature gradient on electric current transport phenomena in semiconductors are discussed and a novel mechanism for this influence is proposed, namely, the heating up of charge carriers under the influence of a large temperature gradient.

3.2 Influence of a Temperature Gradient on Transport Phenomena in Semiconductors

The influence of temperature gradient on charge carriers transport starts to be manifest when characteristic temperature changes become comparable to the mean free path of electrons or to any other characteristic lengths.

The characteristic length L_T of temperature change is equal to[1,2]

$$L_T = \frac{T}{|\nabla T|} \tag{3.1}$$

where ∇T is the temperature gradient.

The following inequalities hold true for the principal microscopic lengths in elastic or quasielastic mechanisms of charge carrier scattering[1,2]:

$$L_r >> L_\varepsilon >> L_p >> L_{ph} \tag{3.2}$$

where L_r is the recombination length, L_ε is the current carrier cooling length, L_p is the momentum mean free path of carriers, and L_{ph} is the thermal phonons mean free path.

With increasing temperature gradient, the length L_T can first of all be comparable to the largest of the lengths in inequalities (Equation 3.2), the recombination length

$$L_r \geq L_T \tag{3.3}$$

Tauc[7] theoretically investigated the case of Equation 3.3 when studying the Benedicks effect. According to the Tauc theory, under the condition of Equation 3.3, the minor current carriers diffusing into the low-temperature region of the sample at a sudden temperature drop are not in equilibrium. This causes a change in the semiconductor properties in the region of large temperature gradients, for example, a change in the thermo-EMF. However, a change in thermo-EMF due to large temperature gradients in

© 2006 by Taylor & Francis Group, LLC

this case proved to be very small and can be completely neglected in materials with a large current carrier concentration.

With further increasing the temperature gradient, the characteristic length L_T can become comparable to the cooling length L_ε:

$$L_T < L_\varepsilon \tag{3.4}$$

In this case, it is natural to expect the appearance of new electron transport phenomena caused by the analogy between strong electric fields and large temperature gradients. It is appropriate to introduce the concept of specific heating of the electron gas in semiconductors under large temperature gradients. Thus, for a homogeneous isotropic semiconductor with a standard band structure the expression for current density in the presence of electric field and temperature gradient is given by the kinetic integrals:

$$\vec{j} = \frac{4n}{3\sqrt{\pi}mT^{5/2}}\left\{\vec{E}\int_0^\infty \varepsilon^{3/2}\tau_p e^{\varepsilon/T}d\varepsilon - \nabla T\left[\frac{\zeta}{T}\int_0^\infty \varepsilon^{3/2}\tau_p e^{\varepsilon/T}d\varepsilon - \frac{1}{T}\int_0^\infty \varepsilon^{5/2}\tau_p e^{\varepsilon/T}d\varepsilon\right]\right\} \tag{3.5}$$

where n, m, ε, and τ_p are the concentration, the effective mass, the energy, and the electron momentum relaxation time, respectively, and ζ is the chemical potential (for simplification of formulas in Equation 3.5 and in all subsequent equations of Chapter 3, we accept the system of units in which the Boltzmann constant $K_B = 1$ and the electron charge $e = 1$).

Provided eddy currents are not present in the case under consideration, in an open circuit an electric field is created:

$$\vec{E} = \left(\frac{\zeta}{T} - n_1 - \frac{5}{2}\right)\nabla T \tag{3.6}$$

where $\tau_p \sim \varepsilon^{n_1}$. Using Equations 3.5 and 3.6 the specific density of partial current (electron current with the energy from ε to $[\varepsilon + d\varepsilon]$) can be written:

$$\frac{d\vec{j}(\varepsilon)}{d\varepsilon} = \frac{4n\tau_p\varepsilon^{3/2}e^{-\varepsilon/T}}{3\sqrt{\pi}mT^{5/2}}\left(\frac{\varepsilon}{T} - n_1 - \frac{5}{2}\right)\nabla T \tag{3.7}$$

It follows from Equation 3.7 that even at zero macroscopic current the partial currents are nonzero, because the difference in the parentheses goes to zero with the only fixed value of ε. As long as the partial currents are temperature dependent, and the temperature depends on coordinate x, the number of ε-electrons entering the element of the sample $[x, x + dx]$ is not equal to the number of ε-electrons leaving the element. Thus, the number of ε-electrons in this element of the sample will change. Consequently, the symmetric part of the distribution function (concerning to the quasimomentum) will also change. The change in the distribution function can be interpreted as specific electrons heat up under large temperature gradients. Naturally, the heating up will be significant if the temperature gradient is large enough.

If the conditions for establishing the electron and phonon temperatures are provided, the nature of the electrons' heat up under large temperature gradients can be also understood from macroscopic considerations.[1,2]

As long as L_ε continues to be the second largest microscopic length in semiconductors next to the recombination length L_r, the investigation of phenomena caused by the heat up of electron gas under large temperature gradients will be of primary practical interest.

The cooling length is also a very important parameter for studying the heat up of electrons; cooling lengths at room temperature for a number of materials are listed in Table 3.1.[1,2] Cooling lengths, as a rule, increase with a decrease in temperature.

© 2006 by Taylor & Francis Group, LLC

TABLE 3.1 Cooling Lengths for Different Materials

Material	L_ε (cm)
Ge	1.7×10^{-4}
Si	5.9×10^{-5}
GaAs	4.0×10^{-4}
InSb	1.0×10^{-4}
BiTe	5.5×10^{-5}
CdS	5.6×10^{-6}
CdSe	2.7×10^{-5}
HgSe	9.1×10^{-4}
GaP	7.1×10^{-6}
InP	2.3×10^{-4}
PbTe	7.7×10^{-5}
HgTe	1.0×10^{-3}
Sn	4.0×10^{-6}
Pb	2.6×10^{-6}
In	5.6×10^{-6}
Cu	2.0×10^{-6}
Ag	2.1×10^{-5}
Au	1.2×10^{-5}

3.3 Calculation of the Influence of a Large Temperature Gradient on the Properties of Semiconductor Materials

Consider a homogeneous, isotropic nondegenerate semiconductor with a standard band structure. To describe the influence of a large temperature gradient, it is necessary to take into account the self-consistent behavior of electron and phonon subsystems and the electric field in the sample. Consider two variants of the problem formulation.

3.3.1 High Current Carrier Concentrations

It is assumed that the current carrier concentration is sufficiently high; i.e., for the current carrier subsystem the electron temperature approximation can be used. The respective inequalities are written in Ref. [8]. Under these assumptions the equations of electron and phonon energy balance can be derived from the original kinetic equations by respective integration[1,2]:

$$\operatorname{div} \vec{q}_e = \vec{j}\vec{E}^* - P(T_e - T_p) \tag{3.8}$$

$$\operatorname{div} \vec{q}_p = P(T_e - T_p) \tag{3.9}$$

where $\vec{E}^* = -\nabla\tilde{\varphi}$, $\tilde{\varphi}$ is the electrochemical potential, T_e and T_p are the electron and phonon temperatures, respectively, and the function $P = P(T_e, T_p)$ is responsible for electron–phonon energy interaction. The obvious form of P function for various scattering mechanisms can be found in Ref. [8]. For electron and phonon densities of heat flow $\vec{q}_{e,p}$ and for current density $\vec{j}$ the phenomenological relations can be used:

$$\vec{j} = \sigma(T_e)\vec{E}^* - \sigma(T_e)\alpha(T_e)\nabla T_e \tag{3.10}$$

$$\vec{q}_e = -\kappa_e(T_e)\nabla T_e + \Pi(T_e)\vec{j} \tag{3.11}$$

$$\vec{q}_e = -\kappa_p(T_p)\nabla T_p \tag{3.12}$$

© 2006 by Taylor & Francis Group, LLC

where $\sigma(T_e)$, $\alpha(T_e)$, $\kappa_e(T_e)$, $\Pi(T_e) = T_e\alpha(T_e)$ are the electric conductivity, the thermoelectric coefficient, the electron thermal conductivity, respectively, and the Peltier coefficient, $\kappa_p(T_p)$, is the phonon thermal conductivity. Equations 3.10 to 3.12 should be supplemented with the current continuity condition in Equations 3.8 and 3.9

$$\operatorname{div} \vec{j} = 0 \tag{3.13}$$

and the system of Equations 3.8 to 3.13 with boundary conditions.

Experimental results[2,8] prove convincingly that the thermal boundary conditions for electrons and phonons can be assigned separately. For this reason sufficiently general thermal boundary conditions have been assumed[8] (in a one-dimensional case):

$$q_{e,p}|_{x=-a} = -\eta^{-a}_{e,p}(T_{e,p} - T_1)|_{x=-a}, \quad q_{e,p}|_{x=a} = \eta^{a}_{e,p}(T_{e,p} - T_2)|_{x=a} \tag{3.14}$$

where $\eta^{\pm a}_{e,p}$ are the phenomenological coefficients of heat exchange depending on conditions in contact areas.

This written system of nonlinear differential equations shown above in the general case cannot be solved analytically. Its analytical solution cannot be obtained even in a single-temperature approximation ($T_e = T_p$) for the simplest boundary conditions.

Assume that the relative temperature drop at the ends of the sample is small compared to the average temperature:

$$\gamma \equiv \frac{T_2 - T_1}{T^*} << 1, \quad T^* = \frac{T_2 + T_1}{2} \tag{3.15}$$

Here, $T_{1,2}$ are determined by the respective boundary conditions (3.14). Under such assumptions the problem can be divided into two parts:

(A) Determination of the electron and phonon temperatures and electric fields in the sample volume. For this purpose the following solution methods were developed and used: the modified method of perturbation theory, the method for direct approximate solution of differential equations, and the iteration method.[9,10] The results obtained by the above methods were checked numerically.

(B) Determination of the electron and phonon temperatures and electric fields in the sample boundary areas. Here the above-mentioned methods were used and the following problems were studied: determination of temperature fields near the interface of two media and heat transfer through thin layers, temperature, and electric fields in planar laminated media.[11,12]

For cases A and B, the temperature distribution of electrons and phonons was obtained.[9–12]

3.3.2 Low Carrier Concentrations

If the current carrier concentrations are not very high, the electron temperature approximation cannot be used; the respective criteria are given in.[8] The kinetic equation for the calculation of electron distribution function f in a one-dimensional approximation is of the form

$$\frac{1}{m} p_x \frac{\mathrm{d}f}{\mathrm{d}x} + E\frac{\mathrm{d}f}{\mathrm{d}p_x} = \tilde{S}_e f \tag{3.16}$$

where the operator $\tilde{S}_e$ combines the interaction of electrons with phonons and point defects.

Expanding the electron distribution function into the Legendre polynomials[2]:

$$f(\vec{p}) = \sum_{l=0}^{\infty} f_l(\varepsilon) P_l(\cos\vartheta) \tag{3.17}$$

where ϑ is the angle between the direction of the electron momentum vector and the axis x.

© 2006 by Taylor & Francis Group, LLC

Expanding all the terms in Equation 3.16 into the Legendre polynomials and using recurrent relationships, the infinite chain of equations which was solved by the iteration method[13] and the variation method[14] can be obtained. The following infinitesimal parameters were used for the average lengths:

$$g_T = \frac{1}{3}\frac{\bar{L}_\varepsilon^2}{\bar{L}_T^2} << 1 \tag{3.18}$$

Both methods provided a possibility to determine the electron distribution function.

3.4 Distribution Function

Both methods for solving kinetic equations enable structurally equivalent equations for the symmetric part of the current carrier distribution function under large temperature gradient. In the first order by parameters 3.18 these can be represented in the form[13,14]

$$f_0^{(1)} = f_0^{(0)}\left[1 + \Psi_1(\varepsilon)\left(\frac{\mathrm{d}T}{\mathrm{d}x}\right)^2 + \Psi_2(\varepsilon)E\frac{\mathrm{d}T}{\mathrm{d}x} + \Psi_3(\varepsilon)T\frac{\mathrm{d}E}{\mathrm{d}x} + \Psi_4(\varepsilon)T\frac{\mathrm{d}^2T}{\mathrm{d}x^2}\right] \tag{3.19}$$

where $f_0^{(0)}$ is the equilibrium Maxwell function, and $\Psi_i(\varepsilon)$ are known functions (presented in Refs. [1,2,13,14]). The resulting distribution function has two principal differences from the equilibrium Maxwell function[1,2,13,14]:

First, it depends on the squares of the local temperature gradient and the gradient of electrochemical potential. Therefore, the distribution function has nonlinear properties.

Second, it also depends on the coordinate derivatives of the temperature gradients and on the electric field. Therefore, the resulting distribution function is of a nonlocal nature; it depends not only on the generalized forces at a given sample point, but also on their values at neighboring points. Obviously, the nonlocality and the nonlinearity of the distribution function will create a series of new effects originating from a sharp spatial inhomogeneity in a temperature field.

3.5 Temperature Fields and Transport Coefficients

All the methods discussed result in equivalent expressions for the electron and phonon temperatures under given thermal boundary conditions. The basic results can be illustrated as a consequence of a mismatch between the electron and phonon temperatures $\Theta = T_\mathrm{e} - T_\mathrm{p}$. It turned out that temperature mismatch in the bulk of a sample can be represented as a sum of three terms $\Theta = \Theta_\mathrm{F} + \Theta_T + \Theta_\mathrm{J}$, where the term Θ_F appears in the absence of electric current and is related only to the processes of thermal conduction (the authors call it "the Fourier mismatch"), Θ_T occurs at the emergence of heat flow and electric current ("the Thomson mismatch"), and Θ_J exists even without a heat flow, but in the presence of electric current (we shall call it "the Joule mismatch"). The analytical form of the temperature mismatch terms and their evaluation can be found in Refs. [1,2,10].

The temperature mismatch in the volume and at the interface of a sample leads to new phenomena which are thermal analogues of the Joule and Peltier effects (Table 3.2).

TABLE 3.2 Analogues of the Joule and Peltier Effects

Electric Current (Density j)		Heat Flow (Density q)	
Sample Volume	Contract of Two Samples	Sample Volume	Contract of Two Samples
Joule effect	Peltier effect	Analogue of Joule effect	Analogue of Peltier effect

© 2006 by Taylor & Francis Group, LLC

Using the distribution function (3.19), analytical expressions for current and heat flow densities at different scattering mechanisms can be obtained. The relations for the flow densities completely determine all transport phenomena in the electron subsystem, taking into account the nonlinear and nonlocal effects, caused by large temperature gradients. Designating any kinetic coefficient by K, and including under K the resistivity ρ, the Peltier coefficient is Π, the thermoelectric coefficient α, the electron heat conductivity κ_e, and also the average electron energy ε. A change in kinetic coefficient K due to a large temperature gradient can be represented in the form[1,2]

$$\delta K_t = \frac{K_t - K_0}{K_0} = U_t\left(u_{tK}^{(1)} G^2 + u_{tK}^{(2)} G\bar{\rho}j + u_{tK}^{(3)} \bar{\rho}^2 j^2\right) \tag{3.20}$$

where K_0 is the kinetic coefficient under small temperature gradient, index t identifies the method of solving ($t = \mathrm{p}, \mathrm{v}, \mathrm{tw}$ for the perturbation theory, variation, and two-temperature methods, accordingly), and $G = (T_2 - T_1)/2a$ is the average temperature gradient. The values of function U_t can be found in Refs. [1,2]; this function has the order of the small parameter (Equation 3.18) $U_t \sim g_T$. The values of numerical coefficients $u_{tK}^{(i)}$ are presented in Table 3.3.

The table gives the values $u_{tK}^{(i)}$ for the cases when nonlocal effects are absent ($\kappa_\mathrm{p} = \text{const.}$) and for the most important case of temperature dependence ($\kappa_\mathrm{p} \sim T^{-1}$). It can be seen that all the three methods give equal signs of corresponding parameters $u_{tK}^{(i)}$, and the variation and two-temperature approaches lead to a full coincidence of numerical values of these parameters.

In contrast to corresponding coefficients of standard theory, the kinetic coefficients in the case being considered depend on the combinations of temperature gradient and current density squares, i.e., they are nonlinear. Second, they are related to high derivatives of temperature with respect to coordinates, and hence they are nonlocal. The nonlinearity and nonlocality of the kinetic coefficients result in a series of deviations from the standard relationships. Thus, the Lorentz factor $L = \kappa_e\rho/T$ is no longer a constant, but becomes a function of current density and coordinate derivatives of temperature. Besides, in the case under consideration the thermoelectric Thomson relation $\Pi = \alpha T$ is not satisfied. The relationship is simultaneously one of the Onsager relations which are valid when there is a linear relation between the flows and the generalized forces. Therefore, under large temperature gradients the Onsager relations are not valid either.

TABLE 3.3 Kinetic Parameters Obtained by Various Methods

Physical Parameter	Method of Solving (t)	$u_t^{(1)}$		$u_t^{(2)}$		$u_t^{(3)}$
		$\kappa_\mathrm{p} = \text{const}$	$\kappa_\mathrm{p} \sim T^{-1}$	$\kappa_\mathrm{p} = \text{const}$	$\kappa_\mathrm{p} \sim T^{-1}$	
ε (average electrons energy)	p	-0.83	0.17	-0.33	-0.33	0.67
	v	-0.5	0.5	-0.75	-0.75	0.5
	tw	-0.5	0.5	-0.75	-0.75	0.5
ρ (resistivity)	p	-0.21	0.26	1.04	1.04	0.61
	v	-0.25	0.25	-0.38	-0.38	0.25
	tw	-1.87	-0.37	-0.37	-0.37	0.75
Π (Peltier coefficient)	p	$-1.43/\alpha$	$2.07/\alpha$	$-0.27/\alpha$	$-0.27/\alpha$	$2/\alpha$
	v	$4.25/\alpha$	$6.25/\alpha$	$-5/\alpha$	$-5/\alpha$	$1/\alpha$
	tw	$-1.5/\alpha - 0.5$	$1.5/\alpha + 0.5$	$-1/\alpha - 0.75$	$-2/\alpha - 0.75$	$0.75/\alpha + 1$
α (thermo-EMF)	p	$0.97/\alpha$	$-0.01/\alpha$			
	v	0	0			
	tw	$-0.75/\alpha$	$0.75/\alpha$			
κ_e (heat conductivity of electrons)	p	-0.76	-0.26			
	v	-7	-7			
	tw	0.25	0.25			

© 2006 by Taylor & Francis Group, LLC

3.6 New Effects

The abnormal thermoelectric effect of EMF generation (or the Benedicks effect) was investigated.[13,15]

The Peltier coefficient under large temperature gradient includes the terms which are linear and quadratic with respect to temperature gradient. Thus, one can speak about the inverse Peltier effect[1,2] when current density changes its direction into the opposite, with invariable temperature field. This is a "pure" effect caused by a large temperature gradient. Because large temperature gradients reduce the symmetry of crystals, tens of new anisotropic thermoelectric, thermomagnetic, and thermal effects come into being.[17–21]

As long as large temperature gradients change all material properties, the material's requirements for thermoelements operating under large temperature gradients also change.[2,22] It turned out that under large temperature gradients the role of thermoelectric figure-of-merit is performed by a new parameter which is a function of temperature gradient.

The heat up of carriers under the influence of large temperature gradients brings about a set of new transport effects: three mechanisms of electron and phonon temperatures mismatch; the heat analogues of the Joule and Peltier effects; the abnormal and inverse thermoelectric effects; and a number of anisotropic effects, etc. The nonlinear and nonlocal effects which have been discussed are obviously manifested in thermoelectric structures with submicron and nanosize inhomogeneities, such as quantum-dimensional objects[3] and thermoelements with point contacts.[4] It is obvious that large temperature gradients are realized in these cases, and a rigorous theory of thermoelectric phenomena should be constructed with regard for the nonlinearity and nonlocality. It is probable that these large temperature gradients are one of the reasons for the reported considerable increase in thermoelectric figure-of-merit.

3.7 The Outlook for Practical Applications

The experimental creation of large temperature gradients with a view to check new effects is rather complicated. A relatively large temperature gradient is formed in a "pin–plane" contacts area (Figure 3.2). This model was used for the experimental investigation of two pure effects caused by large temperature gradients. The abnormal thermoelectric effect of EMF generation (or the Benedicks effect)[13,15] and the inverse thermoelectric effect are generally known.[16] The presence of the inverse thermoelectric effect

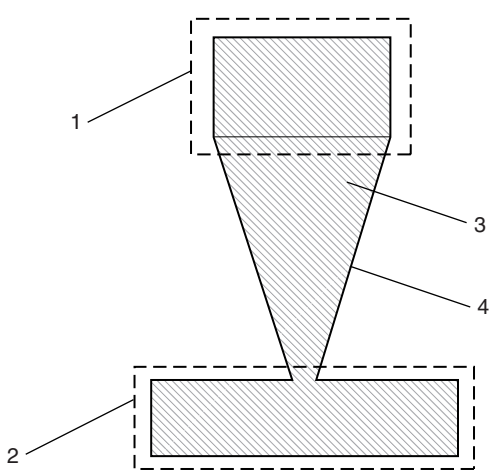

FIGURE 3.2 Scheme of a large temperature gradient formation. 1, 2, thermostats with temperatures T_1 and T_2, respectively; 3, flat homogeneous sample cut along its boundaries 4.

© 2006 by Taylor & Francis Group, LLC

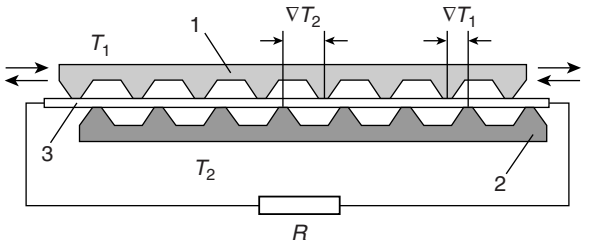

FIGURE 3.3 Scheme of thermoelement with a large temperature gradient and a system of heaters and coolers: 1, periodic system of heaters; 2, periodic system of coolers; 3, thermoelement working medium; R, external load resistance; T_1, heaters temperature; T_2, coolers temperature; ΔT_1, ΔT_2, temperature gradients.

corresponds to transition from the case when temperature gradient and current density in the semiconductor are parallel to the case when they are antiparallel. Such transition causes a change in electric resistivity:

$$\rho(j, \mathrm{d}T/\mathrm{d}x) \neq \rho(-j, \mathrm{d}T/\mathrm{d}x) \tag{3.21}$$

Both effects have been observed in *n-Ge*, the theory being in fairly good agreement with experiment.[15,16]

Thermoelectric devices utilizing the Benedicks effect are of interest.[23] Figure 3.3 shows a linear variant of this thermoelement. A periodic system of heaters and coolers, arranged symmetrically, creates in a semiconductor plate periodic areas with large and small temperature gradients. These thermal conditions provide a series connection of the Benedicks EMF. The system heaters and coolers can move relative to each other. This causes a change in the Benedicks EMF direction and, accordingly, creates another functional dependence of the thermoelement EMF on the motion.

Figure 3.4 is a schematic of a spiral thermoelement utilizing a large temperature gradient. The thermoelement comprises heaters and coolers located on a spiral in pairs. The EMF across the spiral ends is proportional to the number of its coils, the number of pairs of heaters and coolers, the value of the Benedicks effect, which in turn depends on the properties of thermoelectric material, and the magnitude

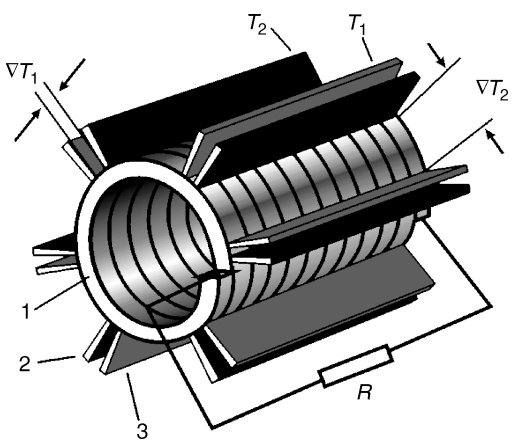

FIGURE 3.4 Scheme of a spiral thermoelement with a large temperature gradient: 1, spiral working medium; 2, cooler; 3, heater; T_1, heaters temperature; T_2, coolers temperature; ΔT_1, ΔT_2, temperature gradients; R, external electric load.

© 2006 by Taylor & Francis Group, LLC

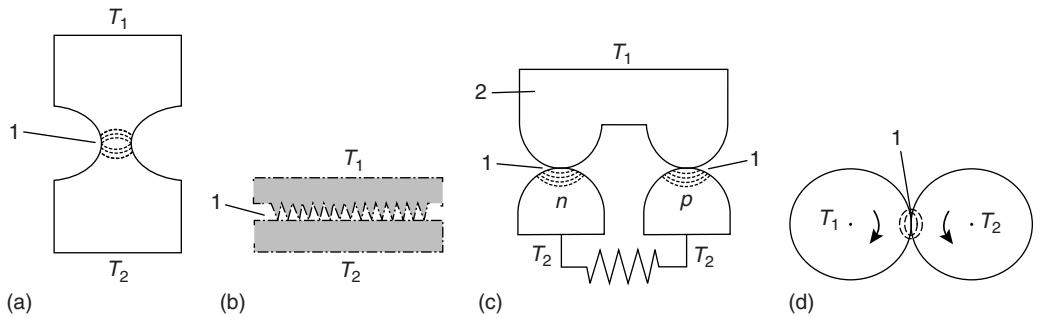

FIGURE 3.5 Models of thermoelements with a large temperature gradient: (1) large temperature gradient region; (a) configuration of module leg with a neck; (b) leg with pressure points; (c) thermocouple with a connecting plate (2) forming a large temperature gradient in contact regions; (d) rotating discs with different temperatures.

of temperature gradient. Because of the absence of connections, such thermoelements are particularly stable in time and can be used in high-precision measuring techniques.

Large temperature gradients can also contribute considerably to a thermoelectric figure-of-merit. A value of $ZT = 1.7$ at room temperature was obtained in thermoelements with pin–plane type point contacts.[4]

A series of patents[5] describe the structures of thermocouple devices used to achieve a large temperature gradient (Figure 3.5). In some of them temperature gradients up to 4.2×10^8 K/cm were achieved. The author of the patents claims that the use of such devices allows efficiency values close to the Carnot cycle efficiency to be achieved.

References

1. Bulat, L.P., *J. Thermoelectricity*, 4, 3–34, 1997.
2. Anatychuk, L.I. and Bulat, L.P., *Semiconductors Under Extreme Temperature Conditions*, p. 224. Nauka, St. Petersburg, 2001.
3. Venkatasubramanian, R., Silvota, E., Colpitts, T., and O'Quinn, B., *Nature*, 413, 597, 2001.
4. Ghoshal, U. *Proceedings of XXI International Conference on Thermoelectrics*, IEEE, p. 540, August 26–29, 2002.
5. Dahlberg, R., *Deutsches Patentamt* 2547262 (22.4.7); 3404137 (8.8.85); 3404138 (8.8.85).
6. Benedicks, M.C., *Acad. Sci. Comptes Rendus.*, 165, 391, 1917.
7. Tauc, J., *Czechosl. J. Phys.*, 6, 108, 1956.
8. Bass, F.G., Bochkov, V.S., and Gurevich, Yu.G., *Electrons and Phonons in Limited Semiconductors*, p. 289. Nauka, Moscow, 1984.
9. Bulat, L.P. and Jatsjuk, V.G., *Fiz. Tverd. Tela.*, 24, 3499, 1982.
10. Bulat, L.P., *Fiz. Tekn. Polupr.*, 21, 1345, see also p. 1347, 1987.
11. Bulat, L.P. and Jatsjuk, V.G., *Fiz. Tekn. Polupr.*, 18, 615, 1984.
12. Bulat, L.P. and Jatsjuk, V.G., *Fiz. Tekn. Polupr.*, 20, 1889, 1986.
13. Bulat, L.P., *Fiz. Tekn. Polupr.*, 11, 2181, 1977.
14. Bulat, L.P. and Tomchuk, P.M., *Solving of Kinetic Equation Under Strong Heterogeneity*, p. 12. Institute of Physics, Kyiv, 1987.
15. Anatychuk, L.I., Bulat, L.P., and Komolov, E.N., *Fiz. Tekn. Polupr.*, 16, 1711, 1982.
16. Anatychuk, L.I., Bulat, L.P., Komolov, E.N., and Ladika, R.B., *Fiz. Tekn. Polupr.*, 18, 342, 1984.
17. Anatychuk, L.I. and Bulat, L.P., Demchishin, E.I., *Dokladi AN USSR (A)*, 5, 42, 1989.
18. Bulat, L.P. and Demchishin, E.I., *Int. J. Electron.*, 73, 881, 1992.
19. Bulat, L.P. and Demchishin, E.I., *Int. J. Electron.*, 76, 805, 1994.

© 2006 by Taylor & Francis Group, LLC

20. Anatychuk, L.I. and Bulat, L.P., *J. Thermoelectricity*, 1, 41, 1998.
21. Bulat, L.P., *Proceedings of XXII International Conference on Thermoelectrics*, IEEE, p. 372, August 17–21, 2003.
22. Bulat, L.P., Buzin, E.V., and Whang, U.S., *Proceedings of XX International Conference on Thermoelectrics*, IEEE, p. 435, June 8–11, 2001.
23. Anatychuk, L.I., *Thermoelectricity*, Vol. 2, Thermoelectric Power Converters, p. 375. Kyiv, Chernivtsi, 2003.

© 2006 by Taylor & Francis Group, LLC